

Graceful Degradation of Air Traffic Operations

Maxime Gariel and Eric Feron

Georgia Institute of Technology Atlanta, GA, 30332-0150, USA

Abstract—The introduction of new technologies and concepts of operation in the air transportation system is not possible, unless they can be proven not to adversely affect the system operation under not only nominal, but also degraded conditions. In extreme scenarios, degraded operations due to partial or complete technological failures should never endanger system safety. Many past system evolutions, whether ground-based or airborne, have been based on trial-and-error, and system safety was addressed only after a specific event yielded dramatic or near-dramatic consequences. Future system evolutions, however, must leverage available computation, prior knowledge and abstract reasoning to anticipate all possible system degradations and prove that such degradations are graceful and safe. This paper is concerned with the graceful degradation of high-density, structured arrival traffic against partial or complete surveillance failures. It is shown that for equal performance requirements, some traffic configurations might be easier to handle than others, thereby offering a quantitative perspective on these traffic configurations' ability to "gracefully degrade". To support our work, we also introduce a new conflict resolution algorithm, aimed at solving conflicts involving many aircraft when aircraft position information is in the process of degrading.

I. INTRODUCTION

Air Traffic Management (ATM) relies on several layers of technology supporting three essential functions: Communication, Navigation and Surveillance (CNS). Advances of the CNS technology base can directly lead to improved air traffic management operations. And indeed, the air traffic management system is left with no choice but to leverage the concurrent advent of digital communication technology, satellite-based navigation and overall improvements of available instrumentation to adjust its ability to handle a fast-growing traffic demand. The resulting Next Generation air transportation systems is described in detail by the Joint Planning and Development Office [1] for US operations, and by the SESAR Consortium [2], [3] for European operations.

For example, one of the cornerstones of expanded operations is ADS-B, a navigation and surveillance concept based on the GPS satellite positioning system which offers the potential for giving pilots more flight autonomy during the en-route flight phase and enabling higher and more flexible traffic densities in terminal

areas. One of the main benefits of ADS-B is to improve navigation precision by providing an accurate position fix. Such technology also enables so-called trajectory-based operations (TBOs), and strategic traffic separation management using the concept of 4-dimensional trajectories (4DTs), whereby an aircraft is able to forecast and broadcast its intended trajectory well before its execution.

However, the obligation for the ATM system to maintain very high reliability and safety levels implies that such new system technologies can be implemented only if they lead to a system with equal or better safety characteristics than currently demonstrated. While system safety includes the ability for the system to operate well under nominal conditions, it is also concerned with off-nominal system behaviors, whereby operations are expected to still remain accident-free for all known failure modes of the system. Failures may affect several parts of the ATM infrastructure:

- **ATM computational infrastructure:** Computers and communication systems (both ground-based and airborne) form the backbone of the air transportation system information infrastructure. Computers are not exempt from such failures, whether the failures involve hardware (motherboard and wiring) or software (incomplete functional requirements or erroneous software implementation).
- **Communications:** A communication mishap can lead to severe consequences. Most lately, on September 25th, 2007, a communication failure at Memphis' Air Route Traffic Control Center (ARTCC) shut down many phone lines, radio communications and radar coverage, completely incapacitating operations for a period of two hours, and despite the presence of about 200 aircraft in the center.
- **Surveillance:** Computer or radar failures can cause surveillance failures. For instance, in December 2000, Miami International airport was subject to repeated radar failures when erroneous flight information data appeared on the controllers' screen. During one such mishap, about 125 flights were rerouted, affecting traffic all over the US.
- **Operations:** For current operation degraded modes, there exist backup procedures described by ICAO in

Graduate Research Assistant, School of Aerospace Engineering, maxime.gariel@gatech.edu

Professor, School of Aerospace Engineering, feron@gatech.edu.

[4]. Also, issues in closely-spaced parallel runway operations is the object of several papers [5], [6]. An analysis of current en route air traffic control usage during special situations can be found in [7]. Operation failures can lead to accidents such as the 2002 crash over Germany between a Russian passenger jet and a cargo plane. Contradictory orders provided by the Traffic Collision Avoidance System (TCAS) and the controller lead to a collision.

- **Vehicles:** An intruder can enter the airspace and consequently, jeopardize the safety of surrounding traffic. A private plane can unintentionally get too close to a restricted airspace such as the vicinity of major airports. If a VFR (Visual Flight Rules) aircraft gets in the landing path of IFR (Instrument Flight Rules) flights, this generates an abnormal situation to be solved by the controller.
- **Airport closure:** An airport or part of it can be closed, e.g for weather conditions. The traffic needs to be reorganized and rerouted towards other airports. For instance, Bangor International Airport is often a diversion destination when freezing rain, snow and fog close Boston, New York or other major Northeast metropolitan centers.

In the past, such failure modes and how to recover from them have been identified on an *ad hoc* basis, whereby accidents have triggered extensive studies and redesigns of the air traffic management operations. Extensive experience about incidents by air traffic controllers has progressively led them to always address “what if” questions during routine operations, leading them to safe operations. This system comes complete with degraded operation and recovery procedures, such as those described in [4]. One example of such fault-tolerant, or fail-safe procedure concerns departure operations: A safe, collision-free path is completely specified to the aircraft prior to take-off, in such a way that the aircraft may follow this path safely even in the case of complete communication failure during take-off.

ADS-B, digital communication technology and advanced automation will enhance higher density airborne operations in the proximity of busy airports, en-route or terminal airspace operations with flexible routes, or cockpit-centric, decentralized conflict management. Those future evolutions of the system will need to be proven fully safe prior to their introduction within the operational landscape. All failure modes will need to be identified and shown to be handled safely prior to the new procedures implementation.

Within this paper, the process by which the current or future system keeps operating safely despite degradation of the sustaining CNS infrastructure will be called “Graceful Degradation”. The term “Graceful Degradation” finds its origins in complex computer systems [8].

However, it can be immediately extended to overall systems such as the National Airspace System (NAS), which include both physical assets (airplanes) and complex information infrastructures. The examination of concepts of operation such as NextGen in the US [1] and SESAR [2], [3] in Europe reveals that system safety and graceful degradation are considered open research issues for most future operations. Tables 1 and 2 present some of the Research and Development topics for SESAR and NextGen, respectively. In many regards, the works that most closely relate to the present paper are those devoted to traffic and airspace complexity [9], [10], [11], [12], [13], [14]. Indeed, these also aim at evaluating, in a broad sense, the resilience of ongoing controlled traffic against off-nominal events.

No	Research topic
15	Study of the following automation topics: Automated separation tools and safety, impact of automation on capacity and impact of loss of situation awareness and tools to manage exceptions associated with loss of situation awareness.
16	Evaluation of ground based de-confliction automation support tools with particular focus on how to ensure feasible solutions with a minimum of constraints on the users trajectory.
41	Evaluation of terminal route structure design involving alternative arrival techniques with multiple or single merging points.
42	Evaluation of Time Based Separation (TBS) on merging points focussing on accuracy requirements and benefits.
49	Study on dynamic risk modelling and management techniques for on-line measurement of safety risk. Study on the assessment of the overall safety of the CONOPS. For now, it is not obvious that the concepts ideas all together are safe in principal (as stated e.g. in Episode 3 objectives).
51	Model complex scenarios of new trajectory based arrival/departure techniques plus existing SID/STAR and also with the SID/STAR from nearby airports plus transit traffic
54	Study controller acceptability of ASAS Spacing versus ASAS Separation during the organization of streams of traffic
62	Development, evaluation and agreement on separation minima for each separation method included in the concept
64	The new separation modes described at least Dynamic Route Allocation, 4D Contracts and ASAS-Self Separation in mixed mode environment shall be assessed with regard to maturity and potential performance: New separation modes shall be assessed with regard to maturity and potential performance: The robustness and stability of the various methods in the face of unexpected events (even of small magnitude) is to be investigated.
80	Elaboration of high density separation concepts and associated airspace issues in terms of detail procedures which should be then validated with a focus on feasibility.

TABLE 1: SESAR R&D topics [3]

In this paper, we are interested in analyzing the conditions for the graceful degradation of high-density traffic when the positioning system substantially degrades.

The motivation behind our work is the widespread and growing implementation of GPS-based ADS-B as a replacement for other, conventional navigation and surveillance mechanisms such as secondary radar and beacon-based positioning systems. Such development offers the potential for enabling higher traffic densities in the vicinity of large and busy airports, enabling “super-density operations”[1]. For that purpose, the remainder of this paper is organized as follows: First, we state the graceful degradation problem in the context of high traffic densities and failing navigation systems. Then, an algorithm of avoidance under uncertainties is used to compare the ability for Miles In Trail and Free flight configurations to manage a loss of accuracy in the positioning system. The avoidance process under uncertainties is analyzed. The algorithm is presented in appendix.

II. GRACEFUL DEGRADATION OF SURVEILLANCE AND NAVIGATION SYSTEMS

This paper focuses on the impact of surveillance and navigation system degradation on aircraft separation requirements. Indeed, the primary mission of the air traffic control system is to ensure safe aircraft separation under all regular and degraded circumstances. Conventional surveillance include radar-based technology, such as primary and secondary radars, and ground-based beacons. New, higher-resolution surveillance systems are enabled by satellite-based positioning systems. Such technologies may enable reduced horizontal separation minima and therefore higher airborne aircraft densities.

We may then formulate the following questions:

- 1) **Analysis: Graceful degradation sensitivity.** *Consider a given air traffic situation (consisting of a number of aircraft with given positions, velocities and headings), what is the “sensitivity” of this situation relative to a sudden degradation of the surveillance system?*
- 2) **Design: Graceful degradation-compatible guidance.** *Consider a set of aircraft with given origins and destinations. Find a sequence of aircraft headings such that the graceful degradation sensitivity of the overall traffic of interest remains below a given threshold.*

In this paper, we will be concerned with the analysis question, leaving the design question for further research. The principle that will drive our analysis can be sketched as follows: Considering a set of aircraft operating under a “high performance” surveillance system, we analyze whether safety can be maintained despite a failure of the surveillance system. Assuming that failures of the surveillance system consist of a partial loss of vehicle coverage, we will be interested in what maneuvers will

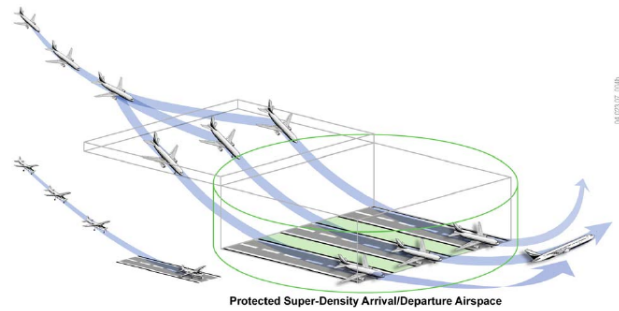


Fig. 1: Super-Density operations [1]

allow aircraft to remain provably separated. Indeed, partial or complete loss of aircraft position coverage results in growing uncertainty about aircraft positions, in such a way that aircraft initially close to each other may not be distinguishable from each other shortly after the failure, unless they maneuver to augment their physical separation. Thus, underpinning our analysis of the the ability for a particular airborne configuration to gracefully degrade, we find the necessity to design procedures enabling traffic to maintain provable separation under degraded conditions. In this paper, such procedure will consist of a novel aircraft conflict management algorithm.

Considering a planar traffic environment for simplicity, we introduce the following definitions:

- 1) **Nominal operations:** *Nominal operations consist of all allowable aircraft operations when aircraft position accuracy is high. The nominal minimum aircraft separation distance (expressed in nautical miles) will be denoted r_0 .*
- 2) **Degraded operations:** *Degraded operation consist of all allowable aircraft operations when aircraft position accuracy is low. The degraded minimum aircraft separation distance (expressed in nautical miles) will be denoted r_f , with $r_f > r_0$.*

Radar precision is one of the main reason for deciding on specific aircraft separation standards. The uncertainty in the position seen by the controllers leads to a separation requirement that can be interpreted as a circle of avoidance around each aircraft. The circle of avoidance corresponds to the area around the aircraft where no other aircraft is allowed. Its radius is generally 2.5 NM for en-route and 1.5 NM for approach. This separation distance ensures safety if the position of the aircraft is relatively well known and regularly updated. Accurate positioning systems such as ADS-B will probably enable a reduction in allowable spacing distance [15]. If a failure happens, the system works in degraded mode, resulting in an increase in uncertainties on the aircraft position observed by the controller. As aircraft’s position are

known less accurately, the resulting radius of avoidance must be increased. The growth of the avoidance circle is limited by backup positioning system (Primary Surveillance Radars, radio...) that enable controllers to get reports on aircraft's position. For instance, in the case of the breakdown of a radar, separation distances must be increased to procedural separation standards [4]. The position of the aircraft will be reported by the pilot to the controller by radio with a low update rate. Between updates, the position of the aircraft is not known and the uncertainty on it increases with time.

In the remainder of this paper, we will assume that a position system failure occurs at time $t = 0$. Prior to that time, nominal aircraft position accuracy will translate into a circle of avoidance with radius r_0 .

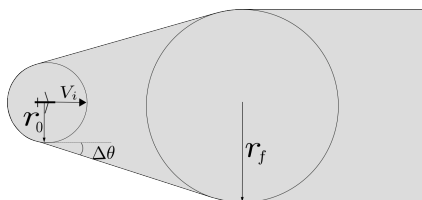


Fig. 2: Track of a growing circle of avoidance

For $t \geq 0$, we propose a time-varying model of position uncertainties, whereby the radius of avoidance grows from r_0 to $r_f > r_0$ over a given period of time. Figure 2 presents the track of a growing circle of avoidance. For instance, r_0 can be the radius of avoidance provided by an ADS-B positioning system, while r_f can be the one provided by a Primary Surveillance Radar (PSR). In the event of an ADS-B failure, the transition from r_0 and r_f must be eventless, in the sense that the transition should not jeopardize the safety of the overall traffic.

For each aircraft i , we will assume a constant growth rate \dot{r}_i , such that $r(t) = r_0 + \dot{r}_i t$. Such a model approximately captures the growing, but bounded uncertainty on aircraft position once the navigation system has failed. Such uncertainty might reflect the effect of uncertainties on the aircraft heading (denoted $\Delta\theta$) and on the aircraft velocity (denoted ΔV_i). Figure 3 shows the uncertainty on the trajectory. A simple way to connect these uncertainties to the growing avoidance radius is to write, for example,

$$\dot{r}_i = \max\{V_i \sin \Delta\theta, \Delta V_i\}. \quad (1)$$

Note this is a conservative approximation.

From these considerations, we see it will not be difficult to create aircraft configurations which are conflict-free, yet will rapidly generate conflicts in case of positioning system degradation. Thus, the ability for such configurations to gracefully degrade will rely on

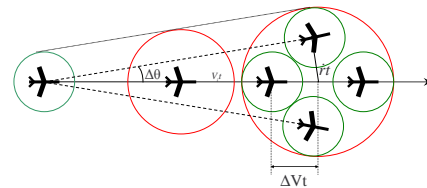


Fig. 3: Uncertainty on the trajectory

our ability to develop a conflict resolution strategy for growing aircraft position uncertainties. Figure 4 shows the difference between a classical conflict avoidance problem and the problem we are solving. In the classical avoidance problem, the radius of avoidance is constant. In our problem, the growing radius of avoidance makes the formulation and resolution more complicated as it is time dependent.

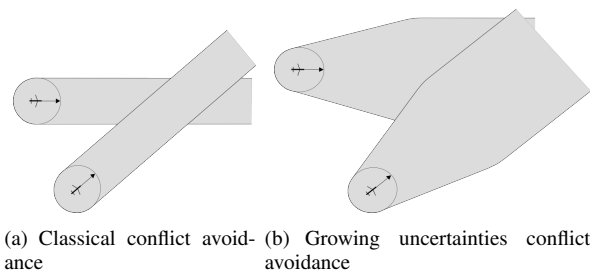


Fig. 4: Conflict avoidance problems comparison

When several aircraft are present within a given airspace sector, the conflict resolution problem under degrading position uncertainty becomes much more complex. An approach using mathematical programming based on a formulation originally presented in [16] is introduced in Appendix. The problem is formulated as a Mixed Integer Linear Program (MILP) and is implemented using the AMPL/CPLEX linear programming tool suite [17], [18].

III. FREE FLIGHT VERSUS MILES-IN-TRAIL ANALYSIS

The parts of airspace where the highest aircraft densities occur are the terminal areas in the vicinity of airports. Therefore, these constitute an ideal setting for evaluating the ability for traffic to undergo graceful degradation. This choice is also motivated by current vistas on future operations in terminal areas, which have been named ‘‘Super-Density operations’’ (NextGen) and ‘‘High Complexity Terminal operations’’ (SESAR). Both consist of increasing the airspace capacity around busy airports. A solution proposed in SESAR [3] is

the multiple merge points arrival operation shown in Figure 5). One way to interpret this solution is to assimilate the new mode of operation to a “Free-Flight” scenario, whereby the route structure in the terminal area is relaxed and the only constraint on incoming aircraft is to meet a specific arrival time at the merge point. This scenario contrasts sharply with current airport arrival practices, where high-density arrival flows of aircraft are organized tens or even hundred of miles prior to landing, by lining up aircraft along arrival routes and spacing them appropriately. Such operations are often denoted Miles-In-Trail (MIT) operations.

Therefore we believe it is interesting and worthwhile to compare the ability for both operations, denoted Free-Flight (FF) and miles-in trail (MIT) to undergo graceful degradation of the navigation system. For that

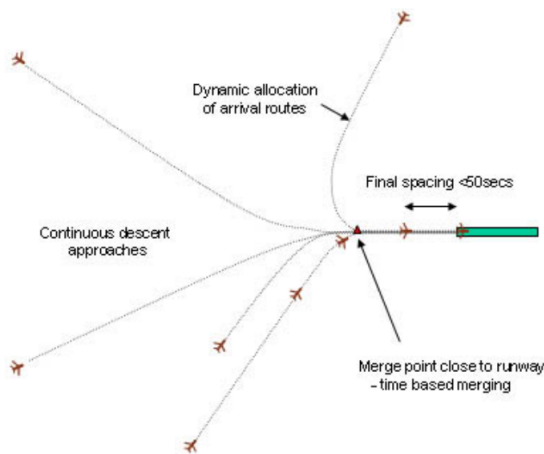


Fig. 5: Arrival Routes, Multiple Merge Points [3]

purpose, we consider a simplified scenario that involve 8 aircraft merging to a common point of coordinates $(0, 0)$. We assume that all aircraft are Time Based Separated (TBS): Each aircraft is given an arrival time so as to meet a precise and regular arrival rate at the merge point. Assuming all aircraft fly at the same speed of 200kt , the aircraft must therefore be initially located on regularly spaced circles centered at the merge point. The inter-aircraft spacings are designed to emulate future Instrument Meteorological Conditions (IMC) arrival operations on closely spaced parallel runways, such as San Francisco Airport: As observed in [19], the average interarrival time for each runway is slightly less than 2 minutes. This translates into a 3Nm average separation between aircraft when they fly at 200kt and the two runways are in use. This separation also turns out to be a *very* conservative estimate of separation requirements for satellite-based navigation systems [15], leading us to an initial circle of avoidance of radius $r_0 = 1.5\text{Nm}$ as proposed by ICAO for ADS-B[20]. The final radius

of avoidance was chosen to be $r_f = 2.5\text{Nm}$ to reflect the surveillance degradation that would occur, should a GPS-based surveillance fail and backup radar-based technology had to be used. The rate of growth reflects a heading uncertainty $\Delta\theta = 5^\circ$. Hence, $\dot{r} = 0.29\text{Nm}/\text{min}$. The transition time between r_0 and r_f is $T = 3.44\text{min}$.

The goal of this study is to evaluate the impact of changing arrival operations from Mile-In-Trail towards Free Flight. For that purpose, we consider an “arrival cone” whose vertex is at the merge point. When the cone’s angular width is zero or takes small values, it corresponds to highly structured Miles-In-Trail operations. When the cone’s angular width is large, it corresponds to less structured, Free-Flight-like operations.

The remainder of our study consists of understanding the impact of the cone angular width and the aircraft initial separations on traffic degradation, should a surveillance system failure occur. The cone angular width was varied from 10° to 60° . The initial aircraft separation, that is, the distance between two consecutive circles, was chosen to be 3.5Nm . 1650 cases with different arrival angles have been simulated. The following procedure has been used to generate the cases: Since we know the distance of each aircraft to the merging point (fixed separation distance), the aircraft initial heading was picked at random, using a uniform probability distribution in the allowed interval ($\pm 5^\circ$, $\pm 10^\circ$, ...). Figure 6 presents two configurations: MIT and FF. The circles represent the avoidance circles (red = FF, black = MIT) and have initial radius 1.5Nm and are centered on the aircraft. The blue line shows aircraft’s heading. Aircraft are represented by a small circle for the MIT configuration and asterisks for FF configuration. The allowed arrival cone for the FF configuration is depicted in light blue.

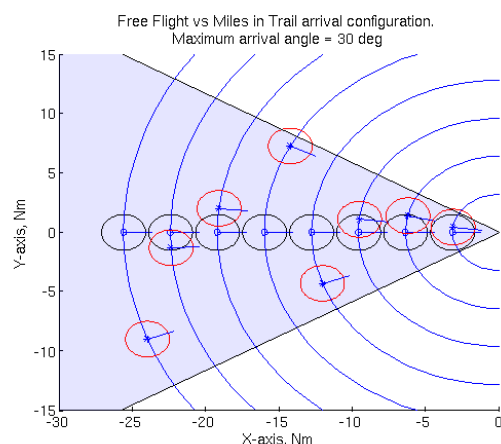


Fig. 6: Free Flight and Miles-In-Trail arrival configurations

To analyze the impact of a surveillance system degradation, these traffic configurations have been used as

initial condition for the conflict resolution algorithm under uncertainties developed in appendix. Let S be the index set of all generated cases. The severity of the traffic management degradation on the traffic situation $s \in S$ was evaluated by measuring the average deviation m_s required for each aircraft, denoting θ_{is0} the initial heading of aircraft i and θ_i its heading after resolution in this situation.

$$m_s = \frac{\sum_{i=1}^n |\theta_{is} - \theta_{is0}|}{n}, \quad (2)$$

where n is the number of aircraft. All the cases were then sorted by absolute value of the maximum aircraft arrival angle and grouped in parameter increments of 2.5° .

$$G_5 = \{s \in S \text{ such that } \max_i \{\theta_{is0}\} \in [0, 5), i = 1 \dots n\},$$

$$G_k = \{s \in S \text{ such that } \max_i \{\theta_{is0}\} \in [k - 1, k), \dots$$

$$i = 1 \dots n\}, k = 7.5, 10, 12.5, \dots, 30. \quad (3)$$

Figure 7 presents the results of the analysis. The maximum deviation m_s experienced within each group was plotted as a function of the corresponding maximum aircraft arrival angle.

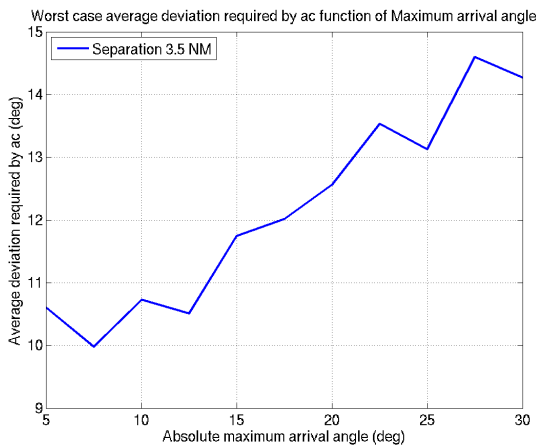
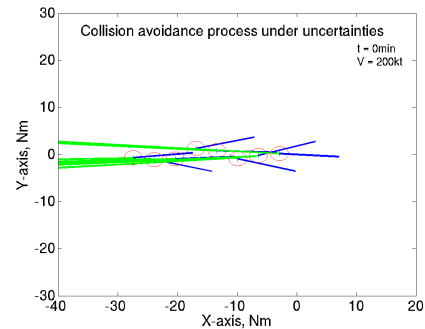


Fig. 7: Evolution of the worst deviation required.

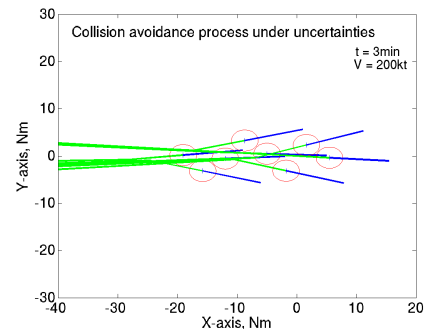
Although the figure suffers from sampling irregularities, the following general trend may be observed: As the arrival cone increases, the aircraft deviations required to ensure a conflict free configuration increases 33%. For an arrival angle less than 5° , the maximum deviation required is 10.6° per aircraft, while it is 14.2° for a maximum arrival angle less than 30° . Figures 8 and 9 show the avoidance maneuvers for the worst cases of G_5 and G_{30} with 3.5NM initial separation. Figure 8(a) and 9(a) present the configuration at $t = 0$. Aircraft are at the position where the avoidance maneuver is calculated. The trajectories of $t < 0$ are represented and the line

pointing out of the aircraft represent the new aircraft's heading.

Free Flight or Miles-In-Trail do not appear to be significantly different from the stand point of surveillance degradation. However, these conclusions were reached using computer-based conflict management which may differ from human-based conflict management.



(a) $t = 0min$



(b) $t = 3min$

Fig. 8: Avoidance maneuvers for the worst case of G_5

IV. CONCLUSION

This paper has outlined the principle of graceful degradation of air traffic operations in the face of Communication, Navigation or Surveillance system failures. Following a generic description of graceful degradation requirements and interpreting it in the context of safety, we have introduced a specific problem of graceful degradation that examines the impact of failures of the surveillance system on airborne traffic separation assurance. Considering current Miles-In-Trail and future Free-Flight approach scenarios, we have shown that free-flight-like airport approaches do not degrade significantly more than current Miles-In-Trail scenarios when facing failures of the surveillance system. During the process of this study, we have developed a new conflict resolution tool that applies to the transient conditions encountered during failures of the surveillance system.

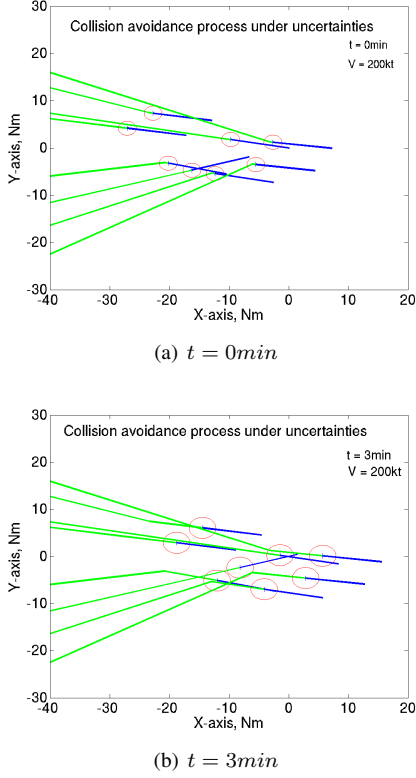


Fig. 9: Avoidance maneuvers for the worst case of G_{30}

APPENDIX

AN ALGORITHM FOR CONFLICT RESOLUTION UNDER UNCERTAINTIES

The following appendix presents the algorithm used to solve the problem of conflict resolution when several aircraft are present. We decided to formulate the problem as a Mixed Integer Linear Program (MILP) as it is an efficient way to solve optimization problems. A typical MILP looks like:

$$\min_{x,z} f_1^T x + f_2^T z \quad (\text{A-1})$$

$$\text{subject to } A_1 x + A_2 z \leq b \quad (\text{A-2})$$

$$(\text{A-3})$$

where $f_1 \in \mathbb{R}^m$, $f_2 \in \mathbb{R}^n$, $x \in \mathbb{R}^m$, $z \in \{0, 1\}^n$. $A_1 \in \mathbb{R}^{m \times m}$, $A_2 \in \mathbb{R}^{n \times n}$, $b \in \mathbb{R}^{m+n}$. In what follows we will focus our attention on developing a MILP model for the conflict resolution problem of interest in this paper.

We consider a set of n aircraft in a planar space. Each aircraft ac_i , $i = 1, \dots, n$ is defined by its position (x_i, y_i) , its heading θ_i and its speed V_i .

The relative velocity V_{ij} and speed V_{ij} of aircraft i with respect to aircraft j , and the distance D_{ij} between

aircraft are given by:

$$V_{ij} = [(V_{x_i} - V_{x_j}), (V_{y_i} - V_{y_j})]^T \quad (\text{A-4})$$

$$= [V_i \cos \theta_i - V_j \cos \theta_j, V_i \sin \theta_i - V_j \sin \theta_j]^T, \quad (\text{A-5})$$

$$V_{ij} = \sqrt{(V_i \cos \theta_i - V_j \cos \theta_j)^2 + (V_i \sin \theta_i - V_j \sin \theta_j)^2}, \quad (\text{A-6})$$

$$D_{ij} = \sqrt{(x_i - x_j)^2 + (y_i - y_j)^2}. \quad (\text{A-7})$$

See also Figure A-1. Let us define some useful parameters for the avoidance problem. Let θ_{ij} be the angle between the relative velocity V_{ij} and the x -axis, ω_{ij} be the angle between the connector of the aircraft and the x -axis. Finally, let γ_{ij} be the angle between the connector of the aircraft and a line starting from aircraft ac_i and tangent to a circle of radius $2r$ and centered at aircraft ac_j . We have:

$$\theta_{ij} = \arctan \frac{V_{y_{ij}}}{V_{x_{ij}}} \quad (\text{A-8})$$

$$= \arctan \frac{V_i \sin \theta_i - V_j \sin \theta_j}{V_i \cos \theta_i - V_j \cos \theta_j} \quad (\text{A-9})$$

$$\omega_{ij} = \arctan \frac{y_j - y_i}{x_j - x_i} \quad (\text{A-10})$$

$$\gamma_{ij} = \arcsin \frac{2r}{D_{ij}}, \quad (\text{A-11})$$

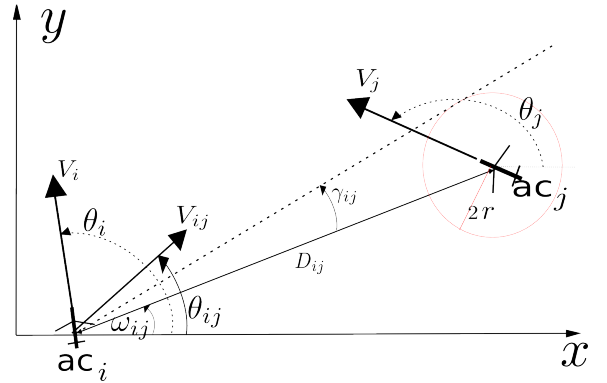


Fig. A-1: Problem configuration

A. Problem structure

We propose to solve the conflict resolution problem arising in this paper using a single heading change. The originality of our problem lies with the fact that the allowable miss distance between the two aircraft is time-dependent. Namely, at time $t = 0$, the minimum miss distance is $2r_0$. For $0 \leq t \leq T$, the minimum miss distance grows from $2r_0$ to $2r_f$. T is given by

$$T = \frac{r_f - r_0}{\dot{r}}, \quad (\text{A-12})$$

where \dot{r} is the growing rate of the circle of avoidance. For $t \geq T$, the miss distance is constant and equal to $2r_f$. Figure A-2 illustrates the conflict avoidance constraint in a relative frame of reference. For no conflict to occur, the circle C of radius $2r_0$ and centered on aircraft ac_j must not intersect the area enclosed by the contour C_2 . This contour C_2 can be seen to be the union of the half line $P1$, the circular segment $P3$ and the line segment $P2$ and their symmetric images across the line passing through ac_i and parallel to the velocity V_{ij} .

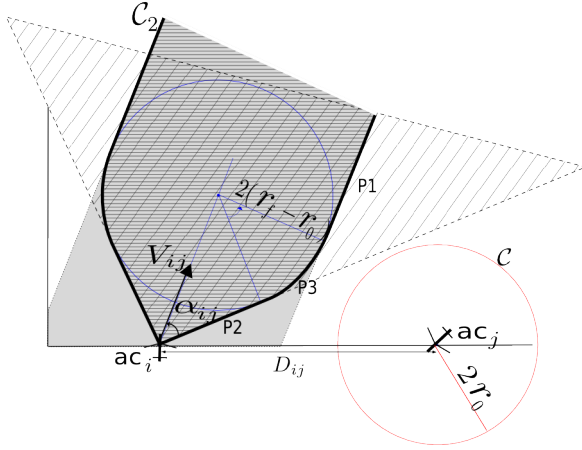


Fig. A-2: Avoidance constraints

For the purpose of linearization, we approximate the contour C_2 by means of line segments, not to be intersected by the circle C . The first, obvious linear approximation is to ask that the circle C not intersect either the gray stripe in figure A-2, or the hatched cone whose vertex is ac_i .

- Asking that the circle C not intersect the gray stripe is a classical conflict avoidance problem that was developed and solved by Pallottino in [16]. This problem deals for time $t \geq T$, when enough time has elapsed for the two radii of avoidance to be equal to r_f . The avoidance problem presented in figure A-2 consists of finding a change in heading for aircraft i and j such that the line parallel to V_{ij} and tangent to the circle of radius $2(r_f - r_0)$ centered on the relative position of aircraft i to aircraft j at T , does not intersect the circle of radius $2r_0$ centered on ac_j . This problem is equivalent to the line directed along V_{ij} and passing by aircraft i does not intersect a circle of radius $2r_f$ and centered on ac_j . The avoidance constraints are then:

$$\begin{cases} \theta_{ij} - \omega_{ij} > \tilde{\gamma}_{ij} \\ \text{or} \\ \theta_{ij} - \omega_{ij} < -\tilde{\gamma}_{ij} \end{cases} \quad (\text{A-13})$$

where

$$\tilde{\gamma}_{ij} = \arcsin \frac{2r_f}{D_{ij}}, \quad (\text{A-14})$$

- Asking that the circle C not intersect the hatched cone can be detailed as follows, referring back to figure A-2. The angular width $2\alpha_{ij}$ of the cone depends on the relative velocity of the aircraft:

$$\sin \alpha_{ij} = \frac{\dot{r}_i + \dot{r}_j}{V_{ij}}. \quad (\text{A-15})$$

If $\dot{r}_i + \dot{r}_j > V_{ij}$, the sum of the radii of the avoidance circles increases faster than the aircraft go away from each other. Whatever the relative velocity, the circles are bound to intersect each other. Hence, the cone of avoidance is the entire plan: as $\arcsin \alpha_{ij}$ is not defined, we set $\alpha_{ij} = \pi$. If $\dot{r}_i + \dot{r}_j = V_{ij}$, the increase rate of the circle of avoidance is the same as the relative speed. Hence, the avoidance cone is a half plane perpendicular to the relative velocity, $\alpha_{ij} = \frac{\pi}{2}$. The distance between the circles of avoidance will remain the same. The

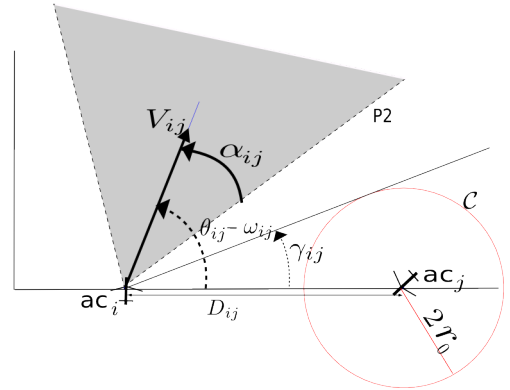


Fig. A-3: Configuration in the relative frame of reference: cone avoidance

condition of avoidance between two aircraft is given by a condition on angles, for $-\frac{\pi}{2} \leq \omega_{ij} \leq \frac{\pi}{2}$:

$$\begin{cases} \theta_{ij} - \omega_{ij} - \alpha_{ij} > \hat{\gamma}_{ij} \\ \text{or} \\ \theta_{ij} - \omega_{ij} + \alpha_{ij} < -\hat{\gamma}_{ij} \end{cases} \quad (\text{A-16})$$

where

$$\hat{\gamma}_{ij} = \arcsin \frac{2r_0}{D_{ij}}, \quad (\text{A-17})$$

Figure A-3 presents those avoidance constraints. To avoid any singularity due to angles around $\pm\pi$, we ensure that $-\frac{\pi}{2} \leq \omega_{ij} \leq \frac{\pi}{2}$. To do so, aircraft are ordered in function of their position (x_i, y_i) so that

we get: $x_1 \leq x_2 \leq \dots \leq x_n$ and if $x_i = x_{i+1}$, $y_i < y_{i+1}$.

The description of the avoidance constraints could be left at that point. However, the developed constraints are somewhat conservative. For example, as shown in figure A-4, the circle C may intersect the cone and the gray stripe without intersecting C_2 . To improve the solution, we may introduce a new constraint. Ideally, we would like to introduce the tangent (ℓ_1) to C_2 at point A. In the relative frame of reference, ℓ_1 has a slope $\theta_{ij} - \frac{\alpha_{ij}}{2}$. ℓ_1 not intersecting C_2 is equivalent to ℓ_3 not intersecting the circle centered on aircraft j and of radius $(2r_0 + |AD|)$. To formulate the constraint, we need the distance $|AD|$, between points A and D. This distance is $2(r_f - r_0) - V_{ij}T \sin \frac{\alpha_{ij}}{2}$. This distance is a non linear function of θ_i and θ_j as V_{ij} and α_{ij} are non linear with respect to θ_i and θ_j . This function depends on too many parameters to be linearized easily. Nevertheless, we can approximate this constraint by using a line ℓ_2 : the line of slope $\theta_{ij} - \frac{\alpha_{ij}}{2}$ passing through a point between A and B. For that, we need to find a majorant to $|DA|$. The following geometrical development gives this majorant: D is the middle of EB and A $\in [DB]$.

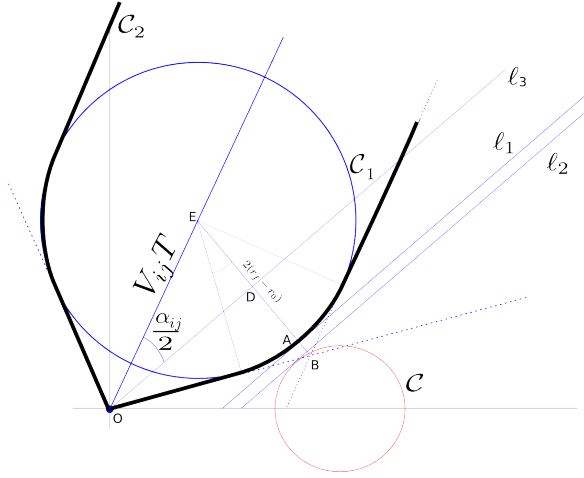


Fig. A-4: Geometry of the curved-part constraint (P3)

$$ED = \frac{EB}{2} \quad (\text{A-18})$$

$$> \frac{EA}{2} \quad (\text{A-19})$$

$$= r_f - r_0. \quad (\text{A-20})$$

Hence, we get

$$DA = EA - ED \quad (\text{A-21})$$

$$< r_f - r_0. \quad (\text{A-22})$$

This leads to the constraint of the line of slope $\frac{\alpha_{ij}}{2}$ not intersecting the circle of radius $2r_0 + \frac{r_f - r_0}{2} = r_0 + r_f$:

$$\begin{cases} \theta_{ij} - \omega_{ij} - \frac{\alpha_{ij}}{2} > \gamma_{ij}^* \\ \text{or} \\ \theta_{ij} - \omega_{ij} + \frac{\alpha_{ij}}{2} < -\gamma_{ij}^* \end{cases} \quad (\text{A-23})$$

where γ_{ij}^* is given by

$$\gamma_{ij}^* = \arcsin \frac{r_0 + r_f}{D_{ij}}. \quad (\text{A-24})$$

As visible on figure A-4, this constraint improves the solution by allowing some solutions where the circle C was intersecting the first two constraints.

B. Optimization of the conflict resolution

In the previous section, we have presented constraints that should be satisfied by the aircraft headings to avoid a conflict. These constraints may be incorporated in an optimal conflict resolution scheme. Denoting the initial heading θ_{i0} of the aircraft i and θ_i its heading after resolution, the problem is to compute:

$$\min J(\theta_1, \theta_2, \dots, \theta_n) = \min \sum_{i=1 \dots n} |\theta_i - \theta_{i0}|, \quad (\text{A-25})$$

subject to

For all aircraft $i = 1 \dots n - 1$,

For all aircraft $j = i + 1 \dots n$

$$\begin{cases} \theta_{ij} - \omega_{ij} > \tilde{\gamma}_{ij} \\ \text{and} \\ \theta_{ij} - \omega_{ij} < -\tilde{\gamma}_{ij} \end{cases}$$

or

$$\begin{cases} \theta_{ij} - \omega_{ij} - \alpha_{ij} > \hat{\gamma}_{ij} \\ \text{and} \\ \theta_{ij} - \omega_{ij} + \alpha_{ij} < -\hat{\gamma}_{ij} \end{cases} \quad (\text{A-26})$$

or

$$\begin{cases} \theta_{ij} - \omega_{ij} - \frac{\alpha_{ij}}{2} > \gamma_{ij}^* \\ \text{and} \\ \theta_{ij} - \omega_{ij} + \frac{\alpha_{ij}}{2} < -\gamma_{ij}^* \end{cases}$$

where $\tilde{\gamma}_{ij}$, $\hat{\gamma}_{ij}$ and γ_{ij}^* , are given by equations A-14, A-17 and A-24, respectively.

C. Identical speeds case

For the sake of computing simplicity, we assume all aircraft share the same speed V . This assumption simplifies the formulae for θ_{ij} and α_{ij} and allows us to obtain piecewise linear approximations.

1) *Expression of the angle of the relative velocity: θ_{ij} :*
Using the assumption of identical speed, the angle between the relative velocity and the x -axis, the expression of θ_{ij} given by equation A-9 can be simplified :

$$\begin{aligned}\theta_{ij} &= \arctan \frac{\sin \theta_i - \sin \theta_j}{\cos \theta_i - \cos \theta_j} \\ &= \arctan \frac{\sin(\frac{\theta_i - \theta_j}{2}) \cos(\frac{\theta_i + \theta_j}{2})}{-\sin(\frac{\theta_i - \theta_j}{2}) \sin(\frac{\theta_i + \theta_j}{2})}.\end{aligned}\quad (\text{A-27})$$

θ_{ij} is a function of $\theta_i + \theta_j$ and $\theta_i - \theta_j$. It can be shown that θ_{ij} is a piecewise affine function of $\theta_i + \theta_j$ and $\theta_i - \theta_j$ of the form $\theta_{ij} = m_{ij}(\theta_i + \theta_j) + p_{ij}$. The value of m_{ij} is always $\frac{1}{2}$ and the values taken by p_{ij} are summarized in table A-1.

We can determine the value of p_{ij} using boolean variables. Let $bCaseDiffPos_{ij}$, $bCaseSumInfmPi_{ij}$, $bCaseSumSupPi_{ij}$, $bCase1_{ij}$ and $bCase4_{ij}$ be boolean variables such that:

$$bCaseDiffPos_{ij} = 1 \iff \theta_i - \theta_j \geq 0 \quad (\text{A-28})$$

$$bCaseSumInfmPi_{ij} = 1 \iff -2\pi \leq \theta_i + \theta_j < -\pi \quad (\text{A-29})$$

$$bCaseSumSupPi_{ij} = 1 \iff \pi \leq \theta_i + \theta_j < 2\pi \quad (\text{A-30})$$

$$bCase1_{ij} = 1 \iff \begin{cases} bCaseDiffPos_{ij} = 0 \\ \text{and} \\ bCaseSumInfmPi_{ij} = 1 \end{cases} \quad (\text{A-31})$$

$$bCase4_{ij} = 1 \iff \begin{cases} bCaseDiffPos_{ij} = 1 \\ \text{and} \\ bCaseSumSupPi_{ij} = 1 \end{cases} \quad (\text{A-32})$$

$$(\text{A-33})$$

Those 3 boolean variables yield the following expression for p_{ij} and hence θ_{ij} :

$$p_{ij} = (bCaseSumPos_{ij} - \frac{1}{2})\pi + 2\pi(bCase1_{ij} - bCase4_{ij}), \quad (\text{A-34})$$

$$\begin{aligned}\theta_{ij} &= \frac{\theta_i + \theta_j}{2} + (bCaseDiffPos_{ij} - \frac{1}{2})\pi + \dots \\ &\quad 2\pi(bCase1_{ij} - bCase4_{ij}),\end{aligned}\quad (\text{A-35})$$

which is linear in θ_i and θ_j and in the boolean variables.

2) *Constraints formulation for θ_{ij} :* The following formulation uses the big- M method. M is a large number such that if multiplied by a boolean set to 1, the constraint is always satisfied, whatever the value of the other variables. This enables us to select between constraints and use *or* relationship between constraints. This is a standard procedure described [21].

Determination of the sign of $\theta_i - \theta_j$:

$$\begin{aligned}bCaseDiffPos_{ij} = 1 &\iff \\ \begin{cases} \theta_i - \theta_j - MbCaseDiffPos_{ij} < 0, \\ -\theta_i + \theta_j - M(1 - bCaseDiffPos_{ij}) < 0. \end{cases}\end{aligned}\quad (\text{A-36})$$

Determination of the boolean $bCaseSumInfmPi_{ij}$ if $\theta_i + \theta_j < -\pi$:

$$\begin{aligned}bCaseSumInfmPi_{ij} = 1 &\iff \\ \begin{cases} \theta_i + \theta_j + \pi - M(1 - bCaseSumInfmPi_{ij}) < 0, \\ -\theta_i - \theta_j - \pi - MbCaseSumInfmPi_{ij} < 0. \end{cases}\end{aligned}\quad (\text{A-37})$$

Determination if $\theta_i + \theta_j \geq \pi$:

$$\begin{aligned}bCaseSumInfmPi_{ij} = 1 &\iff \\ \begin{cases} -\theta_i - \theta_j + \pi - M(1 - bCaseSumSupPi_{ij}) \leq 0, \\ \theta_i + \theta_j - \pi - MbCaseSumSupPi_{ij} \leq 0. \end{cases}\end{aligned}\quad (\text{A-38})$$

Determination of the boolean $bCase1_{ij}$:

$$\begin{aligned}bCase1_{ij} = 1 &\iff \\ \begin{cases} -1.5 + bCaseDiffPos_{ij} - \dots \\ bCaseSumInfmPi_{ij} + 2bCase1_{ij} \leq 0, \\ -0.5 - 2bCaseDiffPos_{ij} \dots \\ + bCaseSumInfmPi_{ij} - bCase1_{ij} \leq 0, \end{cases}\end{aligned}$$

Determination of the boolean $bCase4_{ij}$:

$$\begin{aligned}bCase4_{ij} = 1 &\iff \\ \begin{cases} 1.5 - bCaseDiffPos_{ij} - bCaseSumSupPi_{ij} \dots \\ -2(1 - bCase4_{ij}) \leq 0, \\ -1.5 + bCaseDiffPos_{ij} + bCaseSumSupPi_{ij} \dots \\ -bCase4_{ij} \leq 0. \end{cases}\end{aligned}\quad (\text{A-40})$$

3) *Cone angular width $2\alpha_{ij}$ in the relative frame of reference:* This section presents the formulas to determine the cone angular width $2\alpha_{ij}$ when aircraft share an identical speed. The assumption leads to $\dot{r}_i = \dot{r}$, $i = 1 \dots n$ and

$$\begin{aligned} \alpha_{ij} &= \arcsin \frac{2\dot{r}}{\sqrt{V^2(\cos \theta_i - \cos \theta_j)^2 + V^2(\sin \theta_i - \sin \theta_j)^2}} \\ &= \arcsin \frac{\dot{r}}{V \left| \sin\left(\frac{\theta_i - \theta_j}{2}\right) \right|} \\ &= \arcsin \frac{\tan \Delta\theta}{\left| \sin\left(\frac{\theta_i - \theta_j}{2}\right) \right|} \end{aligned} \quad (\text{A-41})$$

The half cone angular width α_{ij} is given by equation (A-41) and it is a non linear function of $\theta_i - \theta_j$. This function is symmetric about $\theta_i - \theta_j = 0$ and consists of two quasi convex components, separated at $\theta_i - \theta_j = 0$, as shown in Figure A-5. The epigraph of each of these quasi convex components can be approximated by the intersection of linear constraints defined by their slopes a_k and intercepts b_k . Using the big- M method allows us to account for the presence of two disconnected components, and this linearization leads to:

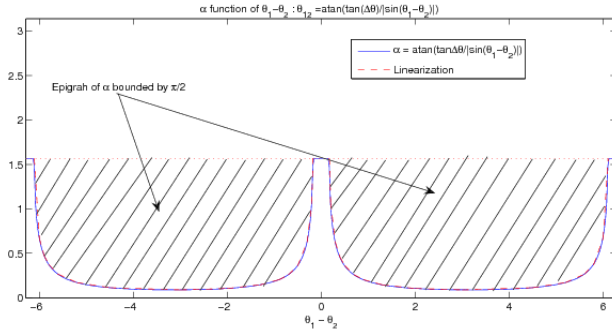


Fig. A-5: α_{ij} function of $\theta_i - \theta_j$ and the linearization used

$$\begin{aligned} a_1(\theta_i - \theta_j) + b_1 - MbCaseAlphaPos_{ij} &\leq \alpha_{ij} \\ a_2(\theta_i - \theta_j) + b_2 - MbCaseAlphaPos_{ij} &\leq \alpha_{ij} \\ &\vdots \\ a_l(\theta_i - \theta_j) + b_l - MbCaseAlphaPos_{ij} &\leq \alpha_{ij} \\ -a_1(\theta_i - \theta_j) + b_1 - M(1 - bCaseAlphaPos_{ij}) &\leq \alpha_{ij} \\ -a_2(\theta_i - \theta_j) + b_2 - M(1 - bCaseAlphaPos_{ij}) &\leq \alpha_{ij} \\ &\vdots \\ -a_l(\theta_i - \theta_j) + b_l - M(1 - bCaseAlphaPos_{ij}) &\leq \alpha_{ij} \end{aligned} \quad (\text{A-42})$$

with $bCaseAlphaPos_{ij}$ a binary variable used to transform the *or* between the constraints in an *and* relationship.

The avoidance constraints are now given by:

$$\left\{ \begin{aligned} &-\frac{\theta_i + \theta_j}{2} - \left(\frac{1}{2} - bCasePlus_{ij}\right)\pi + \omega_{ij} + \alpha_{ij} \dots \\ &\quad + \hat{\gamma}_{ij} - MbCaseIneqPos_{ij} < 0 \\ &\text{and} \\ &\frac{\theta_i + \theta_j}{2} + \left(\frac{1}{2} - bCasePlus_{ij}\right)\pi - \omega_{ij} + \alpha_{ij} \dots \\ &\quad + \hat{\gamma}_{ij} - M(1 - bCaseIneqPos_{ij}) < 0 \end{aligned} \right. \quad (\text{A-43})$$

with $bCaseIneqPos_{ij}$ a binary variable used to transform the *or* between the constraints in an *and* relationship.

4) *Mixed constraints for conflict avoidance:* The conflict avoidance constraints given by equation A-26 can be handled in a linear programming framework by using the big- M method, leading to the following mixed constraints:

$$\left\{ \begin{aligned} &-\frac{\theta_i + \theta_j}{2} - \left(\frac{1}{2} - bCasePlus_{ij}\right)\pi + \omega_{ij} + \tilde{\gamma}_{ijr_0} \dots \\ &\quad - MbCaseIneqPos_{ij} - Mb1_{ij} < 0 \\ &\frac{\theta_i + \theta_j}{2} + \left(\frac{1}{2} - bCasePlus_{ij}\right)\pi - \omega_{ij} + \tilde{\gamma}_{ijr_0} \dots \\ &\quad - M(1 - bCaseIneqPos_{ij}) - Mb1_{ij} < 0 \\ &-\frac{\theta_i + \theta_j}{2} - \left(\frac{1}{2} - bCasePlus_{ij}\right)\pi + \omega_{ij} + \alpha_{ij} + \hat{\gamma}_{ijr_f} \dots \\ &\quad - MbCaseIneqPos_{ij} - Mb2_{ij} < 0 \\ &\frac{\theta_i + \theta_j}{2} + \left(\frac{1}{2} - bCasePlus_{ij}\right)\pi - \omega_{ij} + \alpha_{ij} + \hat{\gamma}_{ijr_f} \dots \\ &\quad - M(1 - bCaseIneqPos_{ij}) - Mb2_{ij} < 0 \\ &-\frac{\theta_i + \theta_j}{2} - \left(\frac{1}{2} - bCasePlus_{ij}\right)\pi + \omega_{ij} + \frac{\alpha_{ij}}{2} + \gamma_{ijr_f}^* \dots \\ &\quad - MbCaseIneqPos_{ij} - Mb3_{ij} < 0 \\ &\frac{\theta_i + \theta_j}{2} + \left(\frac{1}{2} - bCasePlus_{ij}\right)\pi - \omega_{ij} + \frac{\alpha_{ij}}{2} + \gamma_{ijr_f}^* \dots \\ &\quad - M(1 - bCaseIneqPos_{ij}) - Mb3_{ij} < 0 \\ &b1_{ij} + b2_{ij} + b3_{ij} = 2 \end{aligned} \right. \quad (\text{A-44})$$

with $b1_{ij}$, $b2_{ij}$ and $b3_{ij}$ binary variables.

The global algorithm consists on minimizing expression A-25 subject to all the constraints previously developed. We wrote the constraints in an AMPL format and solved using CPLEX. MATLAB was used to generate the 1650 cases and was also used for the post-processing. The computing time to solve an 8 aircraft configuration ranged from less than a second to dozen of seconds on a 4-processor, Pentium class computer.

ACKNOWLEDGMENT

This research was sponsored by Thales Air Systems. The authors would like to thank John Hansman from MIT for useful discussions about parallel approaches.

REFERENCES

- [1] JPDO. Concept of Operations for the Next Generation Air Transportation System. Technical report, Joint Planning and Development Office, June 2007.
- [2] SESAR Consortium. SESAR definition phase, deliverable 3 : The ATM target concept. Technical report, September 2007.
- [3] SESAR Consortium. SESAR concept of operation, milestone 3. Technical report, October 2007.
- [4] ICAO. *Procedures for Air Navigation Services (PANS) - ATM doc 4444*, 14th edition, 2001.
- [5] A. Pritchett, B. Carpenter, K. Asari, J. Kuchar, and R.J. Hansman. Issues in airborne systems for closely-spaced parallel runway operations, 1997.
- [6] Amy R. Pritchett and R. John Hansman. Pilot non-conformance to alerting system commands during closely spaced parallel approaches, 1997.
- [7] FAA DOT. An analysis of en route air traffic control system usage during special situations. Technical report, May 2006.
- [8] M.P. Herlihy and J.M. Wing. Specifying graceful degradation in distributed systems. In *PODC '87: Proceedings of the sixth annual ACM Symposium on Principles of distributed computing*, pages 167–177, New York, NY, USA, 1987. ACM Press.
- [9] R.H. Mogford, JA Guttman, SL Morrow, and P. Kopardekar. The complexity construct in air traffic control: A review and synthesis of the literature, 1995.
- [10] D. Delahaye and S. Puechmorel. Air traffic complexity map based on non linear dynamical systems, 2005.
- [11] K. Lee, E. Feron, and A. Pritchett. Airspace complexity. In *Forty-Fourth Annual Allerton Conference, Allerton House, UIUC, Illinois, USA*, 2006.
- [12] B. Sridhar, K.S. Sheth, and S Grabbe. Airspace complexity and its application in air traffic management. In *2nd USA/EUROPE Air Traffic Management R&D Seminar*, December 1998.
- [13] H.H. Versteegt and H.G. Visser. Traffic complexity based conflict resolution. In *AIAA Guidance, Navigation, and Control Conference and Exhibit*, August 2002.
- [14] M.A. Ishutkina, E. Feron, and K.D. Bilimoria. Describing Air Traffic Complexity Using Mathematical Programming. *AIAA 5 th Aviation, Technology, Integration, and Operations Conference(ATIO)*, pages 1–9, 2005.
- [15] J.D. Powell, C. Jennings, and W. Holforthy. Use of ads-b and perspective displays to enhance airport capacity. In *24th Digital Avionics Systems Conference*, November 2005.
- [16] L. Pallottino, E. Feron, and A. Bicchi. Conflict resolution problems for air traffic management systems solved with mixed integer programming. *Intelligent Transportation Systems, IEEE Transactions on*, 3(1):3–11, 2002.
- [17] R. Fourer, D.M. Gay, and B.W. Kernighan. *AMPL: A Modeling Language for Mathematical Programming*. The Scientific Press Series, 1993.
- [18] ILOG. *CPLEX User's guide*, 1999.
- [19] M. Gariel, J.P. Clarke, and E. Feron. A dynamic I/O model for TRACON traffic management. AIAA, Guidance and Navigation Conference 2007.
- [20] ICAO. ADS-B separation standards under development in the ICAO separation and airspace safety panel (SASP). Technical report, ICAO, 2003.
- [21] F.S. Hillier and G.J. Lieberman. *Introduction to Operations Research*. Seventh edition, 2001.

Ref	Line Reference	Issue
R-6	In addition, backup functions are distributed throughout the system, and there are layers of protection to allow for graceful degradation of services in the event of automation failures.	Develop guidance for what flexibility is allowed in the implementation of airborne separation management algorithms to ensure operationally consistent results, understanding whether variations in algorithms can result in major impacts on overall operations .
R-9	C-ATM is the means by which flight operator objectives are balanced with overall NAS performance objectives and accomplishes many of the objectives for CM, FCM, and TM.	Super Density operations will result in many aircraft in close proximity. Consequently an aircraft deviating from its assigned trajectory is much more likely to cause an immediate conflict with another aircraft, and safe avoidance maneuvers may be limited or unavailable. How can super density operations be conducted safely, especially in the presence of severe weather?
R-10	C-ATM is the means by which flight operator objectives are balanced with overall NAS performance objectives and accomplishes many of the objectives for CM, FCM, and TM.	Develop requirements for a collision avoidance system that is compatible with NextGen tactical separation? Unless mandated otherwise, some aircraft will likely be equipped with legacy TCAS/ACAS systems which may generate unwanted alerts during normal operations. How should this be accounted for?
R-28	In all, these new kinds of flight operations dramatically improve en route productivity and capacity and are essential to achieving NextGen.	If the automation fails, what is the backup plan in terms of people/procedures/automation?
R-44	As illustrated in Figure 1, superdensity corridors handle arriving and departing traffic, while much nearby airspace remains available to other traffic.	We do not prove today's ATC system is safe, but rely on historical data. NextGen will be required to both be safe and to demonstrate it is safe. How will safety be designed into all aspects of NextGen and then proven?
P-1	In addition, backup functions are distributed throughout the system, and there are layers of protection to allow for graceful degradation of services in the event of automation failures.	Develop policies concerning liability for delegated separation and self-separation operations.

TABLE 2: NextGen research and policies issues (Part 2)

Case 1	$\theta_i - \theta_j < 0$ and $-2\pi \leq \theta_i + \theta_j < -\pi$	$p_{ij} = \frac{3\pi}{2}$
Case 2	$\theta_i - \theta_j < 0$ and $-\pi \leq \theta_i + \theta_j < 2\pi$	$p_{ij} = -\frac{\pi}{2}$
Case 3	$\theta_i - \theta_j \geq 0$ and $-2\pi \leq \theta_i + \theta_j < \pi$	$p_{ij} = \frac{\pi}{2}$
Case 4	$\theta_i - \theta_j \geq 0$ and $\pi \leq \theta_i + \theta_j < 2\pi$	$p_{ij} = -\frac{3\pi}{2}$

TABLE A-1: Intercept coefficient of θ_{ij}